Photometric characteristics of haem proteins in erythropoietin-producing hepatoma cells (HepG2)

Agnes GÖRLACH,* Georg HOLTERMANN,* Wolfgang JELKMANN,† John T. HANCOCK,‡ Simon A. JONES,‡ Owen T. G. JONES† and Helmut ACKER*§

* Max-Planck-Institut für Systemphysiologie, Rheinlanddamm 201, 4600 Dortmund 1, Germany, † Physiologisches Institut I, Rheinische Friedrich Wilhelms Universität, Nußallee 11, 5300 Bonn 1, Germany, and ‡ Department of Biochemistry, School of Medical Sciences, University of Bristol, Bristol BS8 1TD, U.K.

Erythropoietin (Epo)-producing hepatoma cells (HepG2) reveal, in addition to the cytochromes of the respiratory chain, a photometrically measurable haem signal with absorbance maxima at 559 nm and 427 nm, suggesting the presence of a *b*-type cytochrome. This activity exhibited a low midpoint potential, CO-binding spectra and reduction which was insensitive to both cyanide and antimycin. This haem possessed a 22 kDa subunit and might be part of an electron transfer chain similar to the NADPH oxidase, since the NADPH oxidase cytosolic activating factor (p47) could be identified by Western blot analysis. H_2O_2, which was detected inside the cells by confocal microscopy, might therefore be produced by the suggested electron transfer chain. This cyanide- and antimycin-insensitive but hypoxia-sensitive cytochrome *b* would be an attractive candidate for controlled Epo production in response to pO_2.

INTRODUCTION

Erythropoietin (Epo) production is triggered in kidney and liver by hypoxia, with the cortical peritubular cells in the kidney being the main source (Koury et al., 1988). The oxygen-sensing process of this hypoxia-mediated hormone production has been intensively investigated at the molecular level in the hepatoma cell lines Hep3B and HepG2 (Goldberg et al., 1988). Both hypoxia and cobalt chloride markedly increase expression of Epo mRNA as well as of biologically active Epo in these cells. Since the increased Epo production under hypoxia could be inhibited by CO, the involvement of a haem protein in the oxygen-sensing mechanism was suggested (Goldberg et al., 1988). A *b*-type cytochrome was proposed as a possible candidate for the oxygen sensor, since phenobarbital, an inductor of cytochrome *P*-450, enhanced Epo production (Fandrey et al., 1990).

To gain further information about the putative oxygen sensor, we investigated the spectral–photometric characteristics of haem proteins in HepG2 cells. Special attention was given to the differences in sensitivity to hypoxia and cyanide or antimycin of intracellular haem proteins, since it has been reported that Epo production can be stimulated by hypoxia but not by cyanide poisoning (Goldberg et al., 1988) or by other inhibitors of the respiratory chain (Tan and Ratcliffe, 1991). We postulate, therefore, that the putative haem protein responsible for the oxygen-sensing process in HepG2 cells should be sensitive to hypoxia only.

MATERIAL AND METHODS

Tissue culture and superfusion of the spheroids

HepG2 cells (ATCC HB 8065) were grown either in monolayer or in multicellular spheroid-tissue culture using the spinner-flask technique (for review, see Acker et al., 1984). For monolayer tissue culture, the HepG2 cells were seeded into 25 cm^2 flasks and grown at 37 °C in Dulbecco's modified Eagle's medium containing 10 % fetal bovine serum in 5 % CO_2 in air. At confluence, the cells were subcultured by 1:5 splits and confluent cells were used between passage numbers 2 and 12. Spheroids were grown in the same medium and under the same temperature and gas conditions in cylindrical spinner flasks (11 cm diam. × 24 cm high), at a spin rate of 40 rev./min. Flasks contained 250 ml of medium, which was replenished twice a week. For photometry and pO_2 measurements, HepG2 multicellular spheroids were used that had a diameter between 500 and 800 μm and contained 17000–66000 cells per spheroid. For this purpose, spheroids were located in a superfusion chamber on a small bench; the bench contained small holes having the same diameter as the spheroids. The superfusion chamber was described in detail elsewhere (Acker et al., 1983); therefore only a brief description is given below. Isotonic salt solution (Locke's solution) containing glucose (5 mM) was equilibrated with different O_2/CO_2 mixtures in order to adjust the pO_2 to various levels, at pH 7.42. The flow rate through the chamber was 10 ml/min. Spheroids were supplied symmetrically with nutrients by this procedure. The temperature was maintained at 36 °C. Oxygen tension, pH and temperature in the Locke's solution were continuously controlled.

Photometry

The superfusion chamber was mounted on the stage of a light microscope (Olympus, Hamburg, Germany) for light absorption measurements. Light from a halogen lamp (12 V, 100 W) transilluminated the spheroid only, since the bench was made opaque by sputtering with gold, which has the advantage of avoiding uncharacteristic light scattering. Light coming from the condensor was guided by the spheroid tissue to the objective. Light was recorded by a photodiode-array spectrophotometer (MCS 210; Zeiss, Köln, Germany), which was connected to the third ocular of the microscope trinocular head via a light guide.

pO_2 measurements

The electrodes used for polarographic pO_2 measurements in the spheroids were single-channel electrodes with a tip diameter of between 2 and 4 μm, and were filled electrolytically with gold

Abbreviations used: Epo, erythropoietin; rh-Epo, recombinant human Epo; DMSO, dimethyl sulphoxide.

§ To whom correspondence should be addressed.

giving a recess of 1–3 μm at the electrode top (Acker et al., 1983). For calibration, pO_2 microelectrodes were introduced into the medium flowing through the chamber by means of a step-driven micromanipulator (Nanostepper, NS 1010; WPI, Frankfurt, Germany). The pO_2 in the medium was then changed by equilibrating the medium with different gas mixtures containing 0%, 10% or 20% O_2 in 5% CO_2; the remaining gas was N_2. Calibration curves were constructed from the polarographic reduction current of the electrode and the different pO_2 values in the medium before and after each measurement in the spheroids. Only results from stable electrodes were considered. The pO_2 microelectrode was positioned on the upper side of the spheroids with a deviation of 15° from the vertical axis for tissue pO_2 measurements with the aid of two independent optical systems (Acker et al., 1983). The electrode was moved stepwise by the micromanipulator towards the centre of the spheroid on a radial trace.

Epo determination

After incubation of HepG2 spheroids for 19 h under control conditions [pO_2 18.67 kPa (140 Torr)], hypoxia [pO_2 1.33 kPa (10 Torr)] or cyanide poisoning (1.5 mM; pO_2 18.6 kPa), cell-free medium was collected by centrifugation at 150 $g \cdot$min. The collected medium was stored at −20 °C. Epo was measured by radioimmunoassay in triplicate according to Fandrey et al. (1990). The assay was carried out using ^{125}I-labelled recombinant human Epo (rh-Epo; 11–33 TBq/mmol; Amersham Buchler, Braunschweig, Germany) and antiserum from a rabbit immunized with rh-Epo. The incubation mixtures each contained 100 μl of cell-free medium, ^{125}I-labelled rh-Epo and antiserum (diluted 1:6000). Calibration curves were obtained with human urinary Epo standards over the concentration range 2.5–250 munits/ml [units calibrated against international standard B (Annable et al., 1972)]. Epo samples were incubated with antibody for 48 h at 4 °C, before ^{125}I-labelled rh-Epo was added for another 24 h of incubation. Then 1 ml of 16% poly(ethylene glycol) 6000 (Merck, Darmstadt, Germany) was added. The radioactivity was measured using a γ-radiation counter (Beckman Instruments Inc., Fullerton, CA, U.S.A.). A log–log plot was applied to calculate the Epo concentration of the samples from the calibration curve. The rate of Epo production was related to the protein content of the spheroids. The lower detection limit of the assay was determined to be 5 munits/ml.

Measurement of H_2O_2 production

Dihydrorhodamine 123 (Molecular Probes, Eugene, OR, U.S.A.) was dissolved in dimethyl sulphoxide to give stock solutions of 50 mM (Cross et al., 1990). The dihydrorhodamine was stored under N_2. The non-fluorescent dihydrorhodamine is converted to rhodamine in the reaction with H_2O_2 inside the spheroids. Images of the fluorescent cells were obtained using a Bio-Rad MRC 500 confocal scanning optical microscope (Bio-Rad, München, Germany) mounted on a Zeiss IM405 inverted microscope (Zeiss, Köln, Germany). For measurements, HepG2 spheroids stained with dihydrorhodamine were placed as described above in the superfusion chamber, which was mounted on the stage of the inverted microscope.

Potentiometric titration

Determination of low-potential cytochrome content was performed as described by Cross et al. (1981). Membrane homogenate from 2×10^6 HepG2 cells suspended in 1.0 ml of 50 mM Mops/100 mM KCl, pH 7.0, was transferred to a cuvette fitted with a platinum electrode and salt-bridge connections to a calomel reference electrode; additions were made by injection through a suba-seal cap and the assembly was gassed with oxygen-free argon. A mixture of mediators (Cross et al., 1981) was added to achieve equilibrium between redox components and the platinum electrode. Potentials were varied by additions of reductant (0.1% sodium dithionite) or oxidant (0.1% potassium ferricyanide). Spectra were recorded while the oxidation–reduction potential in the cuvette was systemically raised and lowered. The proportion of cytochrome *b* reduced at different fixed potentials was calculated using a difference molar absorption coefficient ϵ (558–540 nm) of 21.6 $cm^{-1} \cdot mM^{-1}$.

Western blot analysis with antibodies to the small subunit of cytochrome *b*-245 and to 47 kDa NADPH oxidase cytosolic-activating factor (p47)

Antibodies were a gift from Dr. J. T. Curnutte (Research Institute, Scripps Clinic, La Jolla, CA, U.S.A.) (see Smith and Curnutte, 1991). Proteins from cell homogenates were separated by SDS/PAGE. Proteins were transferred to Hybond enhanced chemiluminescence nitrocellulose by electroblotting at 80 V for 90 min on ice. It was blocked overnight in PBS, pH 7.4, containing 5% (w/v) dried milk and 0.25% (v/v) Tween 20. The blots were washed in buffer (150 mM NaCl, 10 mM Tris, 1 mM EDTA, 0.2% Tween 20, pH 7.5). Primary and secondary antibodies were added in this buffer plus 5% (w/v) dried milk and incubated for 90 min. After washing, plates were developed for 60 s in an equal mixture of Solution 1 plus Solution 2 and exposed to enhanced chemiluminescence Hyperfilm using an ECL Western blotting kit (Amersham Life Science, Aylesbury, Bucks., U.K.). For comparison, HL-60 cells were Western-blotted with anti-p47 antibody; HL60 is a human cell line of primitive myeloid lineage. When incubated in the presence of dimethyl sulphoxide (DMSO), these cells mature from immature promyelocytes to cells that resemble mature granulocytes (Collins et al., 1978). This maturation includes the development of a functional oxidase system, as indicated by enhanced superoxide production, cytochrome *b* induction (Roberts et al., 1982) and hexose monophosphate shunt activity when the cells are stimulated by phorbol 12-myristate 13-acetate (Newberger et al., 1979). HL-60 cells were maintained in culture as described by Newberger et al. (1979), and 1.25% (v/v) DMSO was added to the incubation medium to induce maturation (Collins et al., 1978).

Statistical analysis

Statistical differences were assessed using Student's *t* test. Differences were considered to be significant at $P < 0.05$. Values are given as means ± S.D.

RESULTS

Oxygen supply

To characterize the oxygen supply of the spheroids as the main determinant of Epo production, pO_2 values, measured with microelectrodes inside the spheroid, were collected in a cumulative frequency distribution (Figure 1). The inset shows a typical pO_2 profile inside a single spheroid. When the pO_2 microelectrode was moved towards the spheroids, a decrease in pO_2 became measurable in the superfusion medium. This decrease in pO_2 continued inside the spheroids and reached values of zero at a depth of about 300 μm. A total of 79 measured pO_2

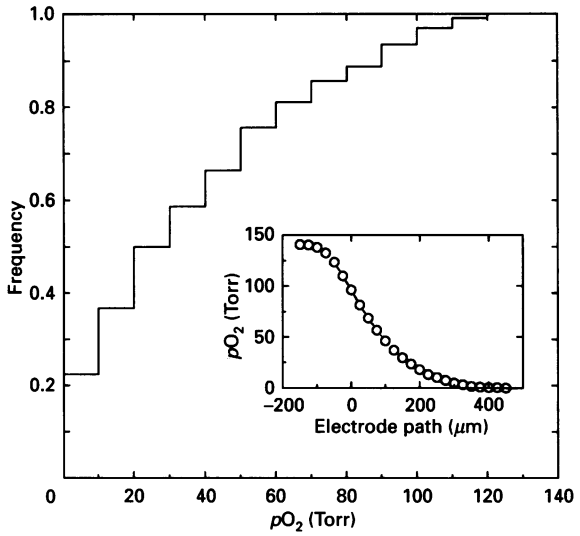

Figure 1 Cumulative frequency distribution of pO_2 in HepG2 spheroids

Over 50% of the values are below 2.67 kPa (20 Torr; 1 Torr = 133.322 Pa). The inset shows a single pO_2 profile in a spheroid with a diameter of 950 μm. A value of 0 μm of the electrode path indicates the surface of the spheroids. Number of spheroids = 4; number of pO_2 values = 79.

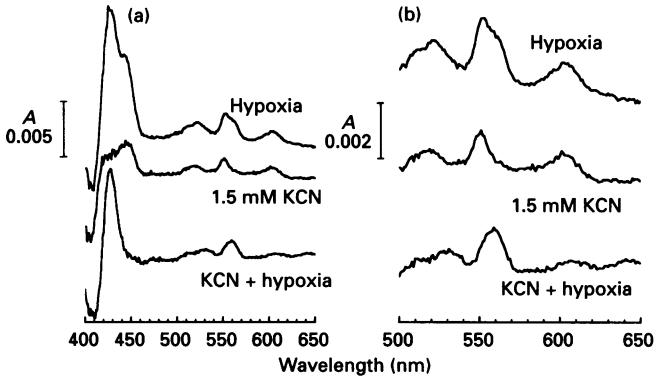

Figure 2 Light absorption difference spectra of one single HepG2 spheroid (a) under hypoxic conditions [pO_2 < 1.33 kPa (10 Torr)] and (b) in the presence of cyanide (1.5 mM)

Panel (**b**) shows in amplified form the wavelength range between 500 and 650 nm of the spectra in (**a**). From top to bottom are shown: hypoxia minus aerobic steady state, aerobic cyanide minus aerobic steady state, hypoxic cyanide minus aerobic steady state.

values from four spheroids were divided into 14 different pO_2 classes (0–10 Torr, 11–20 Torr, ... 131–140 Torr, where 1 Torr = 133.32 Pa), as shown on the x-axis. The frequency of the measured pO_2 values in the different classes was cumulatively registered on the y-axis, showing that 50% of the pO_2 values in the four spheroids were below 2.67 kPa (20 Torr).

Epo production

Epo production in spheroids under control conditions with a pO_2 of 18.67 kPa (140 Torr) in the culture medium was 8.3 ± 3.88 m units/h per mg of protein ($n = 3$). Under hypoxic conditions [pO_2 in the culture medium below 1.33 kPa (10 Torr)] there was a significantly higher value of 27.9 ± 10 m units/h per mg of protein ($n = 3$; $P < 0.05$). Application of 1.5 mM cyanide gave results not significantly different from the control, with a

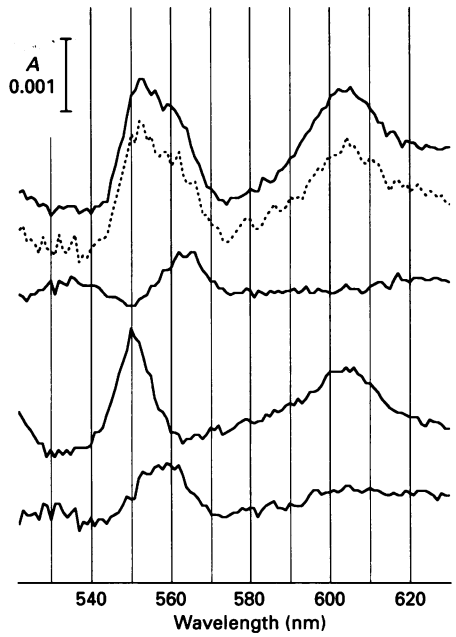

Figure 3 Light absorption difference spectra of one single HepG2 spheroid under hypoxic conditions [pO_2 < 1.33 kPa (10 Torr)], or in the presence of cyanide (1.5 mM) or antimycin (2 μM)

A wavelength range between 520 and 630 nm is shown. From top to bottom are shown: hypoxia minus aerobic steady state, aerobic antimycin minus aerobic steady state, aerobic cyanide minus aerobic antimycin steady state, hypoxia minus aerobic antimycin minus aerobic cyanide steady state. The broken line is a spectrum calculated by summing the last three spectra.

value of 6.1 ± 4.1 m units/h per mg of protein ($n = 3$). Each experiment comprises the Epo production rate of about 150 spheroids.

Haem proteins

Figure 2 shows a typical example of the light absorption characteristics of different haem proteins of one single HepG2 spheroid (diameter 700 μm). A wavelength range of 400–650 nm is shown in Figure 2(a) and a range of 500–650 nm is shown in Figure 2(b). Since the hypoxic cyanide minus aerobic cyanide steady-state difference spectrum revealed a clear peak at 559 nm, indicative of a cyanide-insensitive cytochrome b as described by Jones et al. (1991), antimycin (2 μM) was applied to inhibit the respiratory chain at the b–c_1 complex in an attempt to reveal the cytochrome b peak that is just detectable in the aerobic cyanide minus aerobic steady-state difference spectrum. Figure 3 shows the results with one single spheroid (diameter 750 μm). Inhibition with antimycin revealed a significant peak at 563 nm, indicating the presence of cytochrome b of the respiratory chain (Lemberg and Barrett, 1973), but hypoxia resulted in an additional peak at 559 nm in spite of complete inhibition of the respiratory chain by antimycin and cyanide. The broken line shows a recalculated spectrum that sums the bottom three spectra. This mathematical procedure confirms that the first spectrum is composed of the different haem proteins, as revealed by the use of different blocking agents.

Significantly distinguishable peaks could be identified, as summarized in Table 1, in experiments using HepG2 spheroids as shown in Figures 2 and 3. According to the literature (for a review see Lemberg and Barrett, 1973), peaks at 550 nm and 563 nm can be related to cytochrome c and a mixture of low- and high-potential mitochondrial cytochromes b (see also Nicholls

Table 1 Identified light absorption peaks of difference spectra under different experimental conditions

n = Number of spheroids

Wavelength of peak (nm)			
Hypoxia minus aerobic steady state ($n = 11$)	Aerobic cyanide minus aerobic steady state ($n = 11$)	Hypoxic cyanide minus aerobic cyanide steady state ($n = 11$)	Aerobic antimycin minus aerobic steady state ($n = 5$)
431 ± 0.4		427 ± 1	432 ± 0.2
442 ± 1.3	443 ± 2.5		
551 ± 0.7	550 ± 0.5		
558 ± 0.9	558 ± 0.4	559 ± 1	563 ± 0.5
603 ± 1.4	603 ± 1.4		

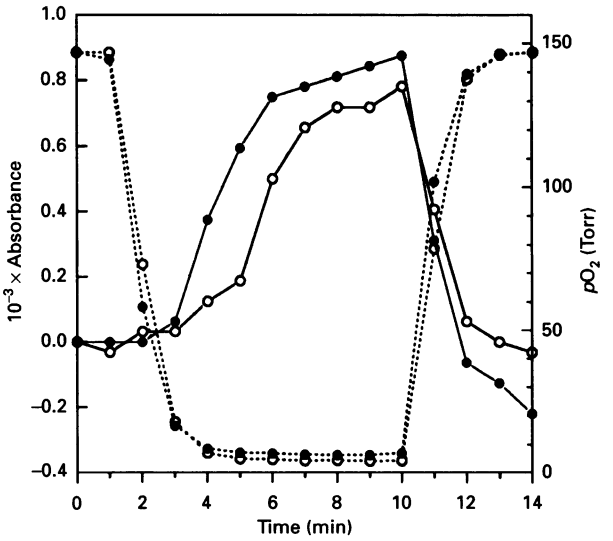

Figure 4 pO_2-dependence of the cyanide-insensitive cytochrome *b* component recorded at 559/575 nm

pO_2 in the superfusion bath is indicated by the broken lines. 1 Torr = 133.32 Pa. The different symbols indicate two different examples.

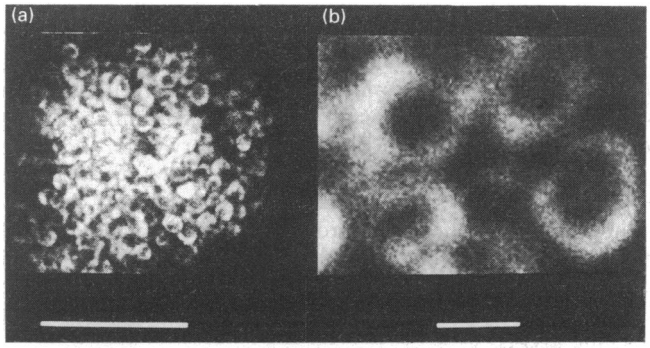

Figure 5 Optical imaging of HepG2 cells in multicellular spheroid culture under control conditions

After incubation with dihydrorhodamine, cells in HepG2 spheroids were stained with rhodamine 123 after the reaction with H_2O_2. (**a**) Surface of a spheroid; (**b**) higher magnification of the cells. Fluorescence intensity is shown with white as highest intensity and black as lowest intensity. Scale bar = 250 μm (**a**) or 25 μm (**b**).

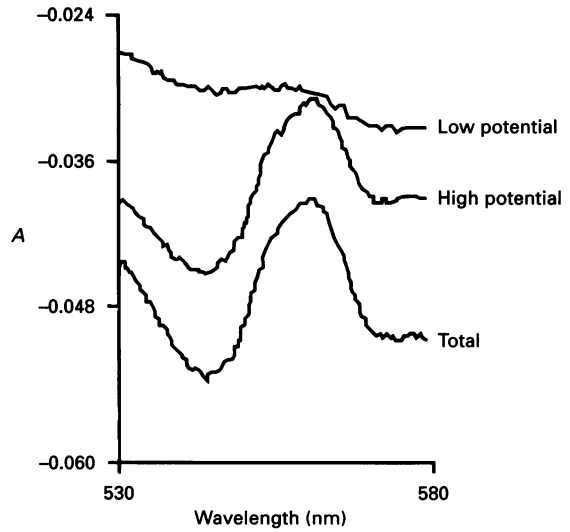

Figure 6 Difference spectra of membrane homogenate from HepG2 cells

Shown are low-potential cytochrome *b* (reduced at −271 mV minus reduced at −141 mV), the high-potential component (oxidized at +236 mV minus reduced at −141 mV) and total cytochromes *b* plus *c* (oxidized at +236 mV minus reduced at −271 mV).

and Ferguson, 1992) respectively, that at 559 nm to the cyanide-insensitive cytochrome *b*, and those at 442 nm and 603 nm to cytochrome aa_3. Figure 4 demonstrates two examples of the pO_2-dependence of the cyanide-insensitive cytochrome *b* component. The figure shows the difference in the absorption changes (maximum versus isosbestic point) at wavelengths 559/575 nm, measured using the dual-wavelength method (Oshino et al., 1974). The differences were calculated from spectra recorded at different time points during the change in pO_2 in the superfusion medium. Cytochrome *b* starts to become reduced at pO_2 values in the superfusion medium below 1.33 kPa (10 Torr). The increase in light absorption at 559 nm under these conditions is 52 ± 18.4% ($n = 7$) of the light absorption increase at 559 nm induced by hypoxia only. Light absorption changes of 44 ± 15.7% ($n = 7$) can be seen at 559 nm by reducing the spheroid tissue with cyanide only.

H_2O_2 production

The confocal microscope scans and collects emitted light only from within the plane of focus of the objective lens (Shotton and White, 1989). Therefore the image obtained is the fluorescence from a discrete slice of about 10 μm within the whole tissue. Non-fluorescent cells are not visible (Cross et al., 1990). Figure 5 shows, at two different magnifications, optical imaging of HepG2 cells in multicellular spheroid culture under control conditions. The highly fluorescent cells are in the plane of the focus. The fluorescent cytosol around the nucleus is clearly visible (Figure 5b). The generation of rhodamine 123 (shown by the fluorescence) suggests that the HepG2 cells in spheroid culture are producing H_2O_2.

Potentiometric difference spectroscopy

By poising the oxidation–reduction potential in the cuvette, it was possible to demonstrate that the HepG2 cells contained an unusual low-potential cytochrome *b*. This appeared in a difference spectrum taken at −271 mV minus −141 mV (Figure 6) and corresponded to approx. 6% of the total cytochrome *b*. A

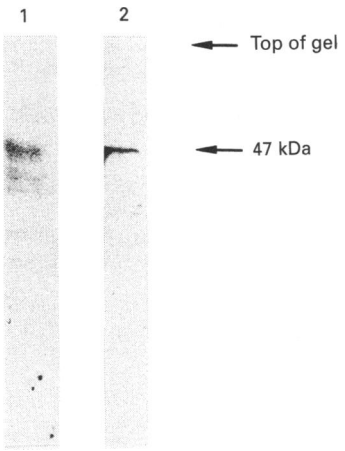

Figure 7 Western blot of HepG2 cells and induced HL-60 cells probed with anti-p47 antibody

Lane 1, 10 μg of HepG2 cells; lane 2, 10 μg of HL-60 cells.

small CO-binding component could be detected in the cytochrome *b* region (559 nm), amounting to 7–8 % of total cytochrome *b* (results not shown).

Western blot analysis of NADPH oxidase components

The potentiometric titration suggested that the HepG2 cells may contain cytochrome *b*-245 (Cross et al., 1981); this is found in large amounts in neutrophils, where it is a component of the NADPH oxidase superoxide-generating system. Cell homogenates probed with antibody to the 22 kDa small subunit of cytochrome *b*-245 (results not shown) and with antibody to p47, an NADPH oxidase-activating protein, both gave weak but positive bands on Western blot analysis. Figure 7 shows the bands of p47 in HepG2 cells and in HL-60 cells.

DISCUSSION

Oxygen radicals and H_2O_2 may be produced by a variety of cytochrome *b*-containing eukaryotic membranes by mechanisms that are CN^--resistant (Cross and Jones, 1991). The cytochrome *b* of the respiratory chain may be involved in a pathway leading to the production of oxygen radicals, consuming up to 5 % of total oxygen uptake. Spectral characteristics published in the literature are in very good accordance with the present results, confirming the specificity of our spectral analysis of the different cytochromes in HepG2 cells (for reviews, see Lemberg and Barrett, 1973, Galeotti et al., 1990). At least two types of cytochrome *b* seem to exist in HepG2 cells. One type, with an absorbance maximum at 563 nm, is classified as a member of the respiratory chain due to its sensitivity to cyanide and antimycin. The other type, with an absorbance maximum at 559 nm, is insensitive to both cyanide and antimycin, indicative of a cytochrome *b* that is a member of an electron transfer chain, such as the NAD(P)H oxidase in neutrophils (Jones et al., 1991). Control difference spectra were recorded in whole-cell suspensions of kidney epithelial cells and colon epithelial cells, as well as in isolated rat liver mitochondria. Using the conditions described in Figures 2 and 3, no hypoxia-specific cytochromes *b* were detected (results not shown). This supports the view that HepG2 cells have a cytochrome *b*-containing electron transport system that is involved in the oxygen-sensing activity of these cells. The relatively low content of low-potential cytochrome *b* found by potentiometric titration (Figure 6) may indicate some unresolved complexity in the sensing system. The results of the potentiometric titration difference spectra and Western blot analysis suggest that HepG2 cells have components in common with the superoxide-generating NADPH oxidase in neutrophils.

The distribution of pO_2 values in HepG2 spheroids, with 50 % below 2.67 kPa (20 Torr), might be a sufficient stimulus for Epo production even under control conditions, at least in the deeper layers of the spheroids. The Epo production in HepG2 cells was unchanged on cyanide application, but could be stimulated by hypoxia (see the Results section). This means that neither reduction of the respiratory chain nor a critical fall in ATP levels serves as a signal for Epo production. Instead, the described cytochrome *b* with a low midpoint potential is an attractive candidate for the control of Epo production, as it is sensitive to hypoxia but not to cyanide. Two previous studies might support the importance of cytochrome *b* in this process. Fandrey et al. (1990) have reported that inducing cytochrome *P*-450, a member of the cytochrome *b* family, by phenobarbital application enhanced Epo production in HepG2 cells. Furthermore, Ueno et al. (1988) have shown that exogenously applied H_2O_2 or glucose oxidase as a direct H_2O_2 generator caused a significant enhancement of Epo production in a renal carcinoma cell line. The participation of H_2O_2 in oxygen sensing has also been suggested in two other systems, i.e. the hypoxic vasoconstriction of lung vessels (Cherry et al., 1990) and pO_2 chemoreception in the carotid body (Cross et al., 1990). In lung vessels, H_2O_2 induces a catalase-dependent guanylate cyclase activation by interaction of the haem groups of the two enzymes, leading probably to a cyclic GMP-mediated opening of K^+ channels with subsequent relaxation of pulmonary arteries. This process is reversed under hypoxia when H_2O_2 production arrests, leading to vasoconstriction (Cherry et al., 1990). The involvement of a cytochrome *b* as a pO_2 sensor has been suggested for the chemoreceptive process in the carotid body (Cross et al., 1990). A spectrophotometric analysis was also carried out in this organ, showing a cytochrome *b* that is sensitive to oxygen but not to cyanide as part of an electron transfer chain able to generate H_2O_2, like the NAD(P)H oxidase in neutrophils (Cross and Jones, 1991). It has been speculated for the carotid body that H_2O_2 production decreases under hypoxia, triggering ion channels by a change in the GSH/GSSG couple (Cross et al., 1990). Future experiments will need to clarify by which mechanism H_2O_2 is regulated under hypoxia in HepG2 cells, and whether H_2O_2 can directly interact with the gene responsible for Epo production (Goldberg et al., 1991).

We thank Brigitte Bölling and Evelyne Dufau for their excellent and skilful assistance in cell culturing and photometric analysis. This work was financially supported by grant 0319417A, BMFT, Bonn/F.R.G. We also thank the Wellcome Trust for their support.

REFERENCES

Acker, H., Holtermann, G., Carlsson, J. and Nederman, T. (1983) Adv. Exp. Med. Biol. **159**, 445–462

Acker, H., Carlsson, J., Durand, R. and Sutherland, R. M. (1984) Recent Res. Cancer Res. **95**, 1–183

Annable, L., Coles, P. M. and Mussett, M. V. (1972) Bull. WHO **47**, 99–112

Cherry, P. D., Omar, H. A., Farrell, K. A., Stuart, J. S. and Wolin, M. S. (1990) Am. J. Physiol. **259**, H1056–H1062

Collins, S, J., Tuscetti, F. W., Gallagher, R. W. and Gallo, R. C. (1978) Proc. Natl. Acad. Sci. U.S.A. **75**, 2458–2462

Cross, A. R. and Jones, O. T. G. (1991) Biochim. Biophys. Acta **1057**, 281–298

Cross, A. R., Jones, O. T. G., Harper, A. M. and Segal, A. W. (1981) Biochem. J. **194**, 599–606

Cross, A. R., Henderson, L., Jones, O. T. G., Delpiano, M. A., Hentschel, J. and Acker, H. (1990) Biochem. J. **272**, 743–747
Fandrey, J., Seydel, F. P., Siegers, C. P. and Jelkmann, W. (1990) Life Sci. **47**, 127–134
Galeotti, T., Borello, S. and Masotti, L. (1990) Oxygen Radicals: Systemic Events and Disease Processes (Das, D. K. and Essman, W. B., eds.), pp. 129–148, S. Karger AG, Munich
Goldberg, M. A., Dunning, S. P. and Bunn, H. F. (1988) Science **242**, 1412–1415
Goldberg, M. A., Imagawa, Sh., Strair, R. K. and Bunn, H. F. (1991) Semin. Hematol. **28**, 35–41
Jones, O. T. G., Cross, A. R., Hancock, J. T., Henderson, L. M. and O'Donnell, V. B. (1991) Biochem. Soc. Trans. **19**, 70–72
Koury, St. T., Bondurant, M. C. and Koung, M. J. (1988) Blood **71**, 524–527
Lemberg, R. and Barrett, J. (1973) in Cytochromes (Lemberg, R. and Barrett, J., eds.), pp. 17–122, Academic Press, New York
Newberger, P. E., Chovaniec, M. E., Greenberger, J. S. and Cohen, H. J. (1979) J. Cell Biol. **82**, 315–322
Nicholls, D. G. and Ferguson, S. T. (1992) Bioenergetics **2**, 107–136
Oshino, N., Sugano, T., Oshino, R. and Chance, B. (1974) Biochim. Biophys. Acta **368**, 298–310
Shotton, D. and White, N. (1989) Trends Biochem. Sci. **14**, 435–439
Smith, R. M. and Curnutte, J. T. (1991) Blood **77**, 673–686
Tan, Ch. C. and Ratcliffe, P. J. (1991) Am. J. Physiol. **261**, F982–F987
Ueno, M., Brookins, J., Beckman, B. S. and Fisher, J. W. (1988) Biochem. Biophys. Res. Commun. **15**, 773–780

Received 20 May 1992/1 October 1992; accepted 22 October 1992